2022 9th IEEE RAS/EMBS International Conference for Biomedical Robotics and Biomechatronics (BioRob) | 978-1-6654-5849-8/22/$31.00 ©2022 IEEE | DOI: 10.1109/BIOROB52689.2022.9925508

Modeling and Design of Soft, Positive-Pressure Actuated Suction Cups for Anchoring in Minimally Invasive Surgery

Ayush Giri[1], Cédric Girerd[1], Xiaolei Luo[1], Ryan Broderick[2] and Tania K. Morimoto[1,2]

***Abstract*—Soft suction cups have been proposed for many applications, including manipulating soft tissues and measuring mechanical properties of the skin. Models that can predict the attachment behavior of such suction cups on their target substrates can help to enable efficient and systematic design. In this work, we develop a finite element model that correctly predicts the attachment behavior of positive-pressure actuated suction cups on both soft and rigid substrates. The model is used in an optimization study to determine a suction cup design that maximizes the attachment force. We propose to use positive-pressure actuated suction cups for anchoring and stabilizing flexible surgical tools during minimally invasive surgery. The optimized suction cup's ability to resist external forces on rigid and soft substrates and on live porcine tissues is evaluated. It is found that the suction cup could resist up to 3.34 N of normal force and up to 1.59 N of shear force on certain porcine tissues, demonstrating its potential as an anchoring unit for surgical applications.**

***Index Terms*—Soft Sensors and Actuators, Soft Robot Materials and Design, Medical Robots and Systems.**

I. Introduction

Soft suction cups have been proposed for a wide range of robotic systems, including for wall climbing robots [1], [2], tissue manipulators [3], and grippers [4], [5], for example. These suction cup designs can be broadly classified as active or passive based on the use or lack of actuation mechanism, respectively [6]. While passive suction cups have relatively simple designs, they require external forces to attach and detach from a substrate, making it difficult to control their adhesion states. In addition, the attachment force provided by a passive suction cup is difficult to regulate. In contrast, the adhesion state and attachment force can be easily controlled in active suction cups, making them more well-suited for interactions with fragile objects or in sensitive environments, such as in Minimally Invasive Surgery (MIS). Different actuation mechanisms, including dielectric elastomers [7], magnets [3], vacuum pressure [8], [5], [9], and positive pressure [10], have been explored for actuating soft suction cups.

Among the several actuation mechanisms, vacuum actuation has been the most heavily explored because these suction cups are simple in design [11] and can hold large loads [12]. However, vacuum actuated suction cups may pose a challenge for use in minimally invasive surgeries (MIS) where CO_2 insufflation is commonly used to help expand the workspace and provide better visibility during procedures [13], [14], since a vacuum could result in the loss of insufflation.

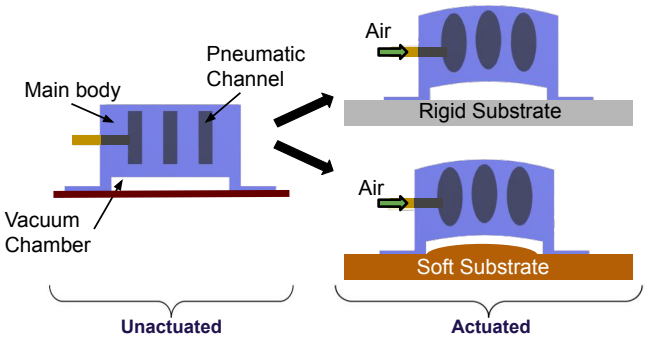

Fig. 1. Schematic showing the cross-section of a positive-pressure actuated suction cup on rigid and soft substrate before and after positive pneumatic load is applied to the pneumatic channel.

In contrast, recently developed positive-pressure actuated suction cups [10] offer several potential advantages. These suction cups consist of a pneumatic channel embedded inside the main body, and a cavity, or vacuum chamber, between the body and the substrate, as shown in Fig. 1. When positive pneumatic load is applied, the channel inflates, causing the body to bend away from the substrate. The increase in volume in the vacuum chamber results in a pressure difference that leads to a suctioning effect. Such suction cups operate without drawing in fluid or contamination from the environment. The switchable adhesion also allows them to easily attach and detach from the substrates [10]. These advantages make positive-pressure actuated suction cups good candidates for use in demanding applications such as surgical procedures.

In addition to recent progress in novel suction cup design, there has also been developments in modeling their behavior [15], [16]. Finite Element Analysis (FEA) was used in [17] to model the deformation of clingfish-inspired passive suction cups on rigid substrates. Similarly, a simplified analytical model was presented in [10] to model the adhesion of a positive-pressure actuated suction cup to a rigid substrate. However, the presented model requires design-specific parameter identification on a physical prototype, and therefore cannot be used for large-scale optimization studies. Moreover, while suction cup designs have been proposed for applications on soft substrates such as skin and tissues [4], [18], studies to date have been limited to attachment on rigid substrates. In order to enable systematic design of soft suction cups for many of these real-world applications, including MIS, it is therefore critical to develop an approach for understanding their interaction with soft substrates.

[1]Department of Mechanical and Aerospace Engineering, University of California, San Diego, La Jolla, CA 92093 USA. aygiri@eng.ucsd.edu

[2]Division of Minimally Invasive Surgery, Department of Surgery, University of California, San Diego, La Jolla, CA 92093 USA.

The contributions of this work are as follows. (1) We present and experimentally validate a finite element model that enables the simulation of the behavior of positive-pressure actuated suction cups on both rigid and soft substrates. This model allows us to estimate the attachment force of the suction cups and to study the non-intuitive behavior of a wide range of designs for optimization purposes. (2) We design a positive-pressure actuated suction cup to anchor flexible surgical tools to surrounding tissues to help stabilize them during procedures. We identify a design that provides maximum attachment force and conduct experimental evaluations to characterize its performance on rigid and soft substrates. Finally, we perform an in-vivo demonstration on porcine liver and spleen that illustrates the ability of the suction cup to resist external forces and its potential to be used as an anchoring unit for surgical tool stabilization.

The paper is structured as follows: we present our modeling and optimization approach for positive-pressure actuated suction cups in Section II. In Section III, we then apply the proposed approach to the design of a suction cup for use in MIS. We fabricate and evaluate the performance of the suction cup with and without external loads on rigid and soft substrates in Section IV and on live porcine tissues in Section V. Finally, we present the conclusion and perspectives in Section VI.

II. Modeling and Optimization Approach

In this section, we present the operating mechanism of positive-pressure actuated suction cups, and propose an FEA implementation to model their behavior. The developed model is then integrated in an optimization approach, which allows us to select designs based on a desired performance metric.

A. Operating Mechanism

Positive-pressure actuated suction cups [10] consist of an embedded pneumatic channel that, when pressurized, causes the main body of the suction cup to bend away from the substrate (see Fig. 1). The volume of the vacuum chamber, which is located beneath the main body, therefore increases by ΔV, leading to a pressure difference, ΔP, between the vacuum chamber and the environment, as shown in Fig. 2. As stated by Boyle's law, this change in pressure is given by

$$\Delta P = P_o \left(\left(\frac{V_o}{V_o + \Delta V} \right) - 1 \right), \tag{1}$$

where P_o is the pressure in the environment and V_o is the initial volume inside the unactuated vacuum chamber. In the absence of external loads, ΔP gives rise to an attachment force, which can be calculated as

$$F = \Delta P \cdot A, \tag{2}$$

where A is the base area of the deformed vacuum chamber. We approximate the base area of the vacuum chamber after actuation to be equal to that before actuation, which is a valid assumption provided the base of the suction cup remains attached to the substrate during actuation, and does not deform. We ensure that the base remains attached to the substrate by adding a thin lip at the base of the suction cup to maintain a proper seal.

B. FEA Modeling

FEA can be accurately used to study the intrinsic nonlinear behavior exhibited by soft materials [19]. We used COMSOL Multiphysics (COMSOL, Inc., Burlington, USA) to develop a finite element model that is used to estimate the achievable attachment force of a suction cup for a given pneumatic load, as shown in Fig. 2. We implemented the parameterized suction cup model illustrated in Fig. 3, with the following design

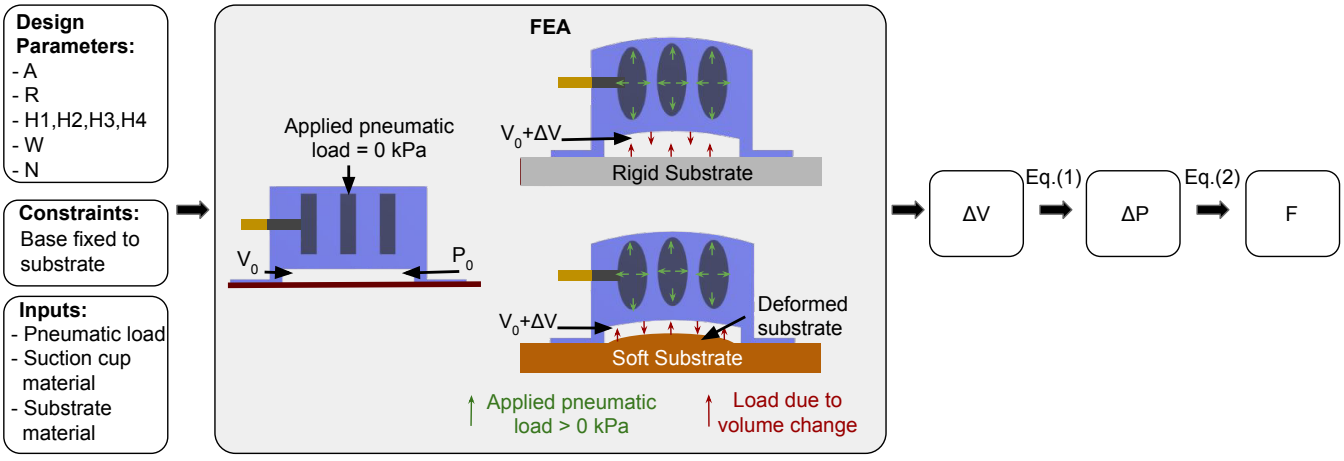

Fig. 2. Proposed workflow for calculating the attachment force of a suction cup design. A suction cup is modeled using the provided geometric parameters and constraints. When a positive pneumatic load is applied in the pneumatic channel, the volume in the vacuum chamber of the suction cup increases from an initial value, V_0, by an amount, ΔV. The achieved ΔV depends on both the magnitude of the applied pneumatic load and on the selected substrate material, since a soft substrate deforms due to the load generated in the vacuum chamber. The obtained ΔV is then used to calculate ΔP, the generated pressure difference, and F, the attachment force, using Eq.1 and Eq.2 respectively.

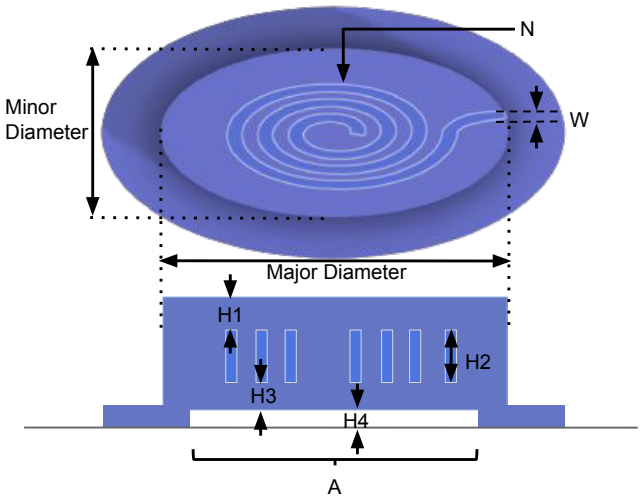

Fig. 3. Top view (top) and cross-sectional view (bottom) of a suction cup with its geometric parameters.

parameters: aspect ratio (R), which is the ratio between the major and minor diameters of the main body, spiral channel width (W), number of revolutions in the spiral channel (N), base area of the vacuum chamber (A), and thicknesses H1, H2, H3 and H4. These design parameters are reported in Fig. 3. The channel that receives the input pneumatic load was selected to be an Archimedean spiral, similar to previous work [10], but alternative designs could be incorporated into the model in future work.

We constrained the bottom surface of the suction cup to be fixed relative to the substrate, assuming that, in practice, the seal is maintained and does not deform during actuation, as described previously. The input pneumatic load, responsible for the actuation of the suction cup, is applied to the walls of the embedded channel. The change in volume, ΔV, generated in the vacuum chamber during actuation also results in a load on the encapsulated walls of the vacuum chamber as shown in Fig. 2, and we have included this resulting load in our simulation as well.

Finally, the material of the substrate can be selected, in order to simulate a desired rigid or soft substrate. If the substrate is soft, it is also subjected to deformations due to the load resulting from the volume change in the vacuum chamber. To account for the resultant deformation of the soft substrate, an accurate material model of the substrate is required. The resultant deformation of the soft substrate along with the deformation of the encapsulated walls of the vacuum chamber result in the corresponding increase in volume in the vacuum chamber, ΔV. The attachment force of the suction cup, F, on both rigid and soft substrates can then be calculated as shown in Fig. 2.

C. Optimization Approach

Since the formulation of a mechanics-based model to describe the behavior of suction cups is difficult in the presence of soft materials, our optimization approach consists of a systematic evaluation of a wide range of suction cup designs using the workflow shown in Fig. 2. The suction cup design with the largest attachment force is determined to be the optimized suction cup design. In order to formulate the set of designs to be studied, considerations in terms of geometry and scale are made with regard to the targeted application. This approach enables the selection of ranges for the design parameters, which includes the aspect ratio, number of revolutions in the spiral channel, base area of the vacuum chamber, spiral channel width, and thicknesses, as detailed previously. Each design parameter is then discretized within its selected range using a chosen step size. The set of step sizes selected should ensure that there are a sufficiently high number of designs in order to capture performance trends, while remaining computationally tractable.

III. Application for Minimally Invasive Surgery

In this section, we use the developed finite element model and apply our optimization approach in order to obtain the design parameters of a suction cup for our target application. We focus here on improving the stabilization of flexible surgical tools during MIS. Large forces can often be involved at the distal end of these tools, leading to unintended bending and deflections of the surgical tool and target tissue that increase the control difficulty [20], [21]. The goal is to design a suction cup capable of providing the largest attachment force, while remaining within the necessary size constraints of the application. We hypothesize that the suction cup's ability to resist external forces is directly correlated to its attachment force in the absence of external loads. The attachment force, F, is thus the selected metric considered for evaluating suction cup performance.

A. Design Requirements and Parameter Selection

Based on the selected application and associated design constraints, we determined the range of values (see Table III) for each design parameter as follows.

Area (A): As shown in Eq. (1), the attachment force is directly proportional to the area A. Thus, area, A, was kept constant across all our designs to enable a fair comparison. It was selected to be equal to that of a circle with a diameter of 25 mm. This pre-selected area ensures that the suction cup is small enough to attach to the surgical tools.

TABLE I
Design Parameters and Their Corresponding Dimensions Considered for the FEA Optimization Study.

Parameter	Min	Max	Step size
A (mm^2)	490.87	490.87	–
H1 (mm)	1.00	4.00	0.50
H2 (mm)	1.00	4.00	0.50
H3 (mm)	1.00	4.00	0.50
H4 (mm)	1.00	4.00	0.50
W (mm)	1.00	1.30	0.15
N	2.75	2.75	–

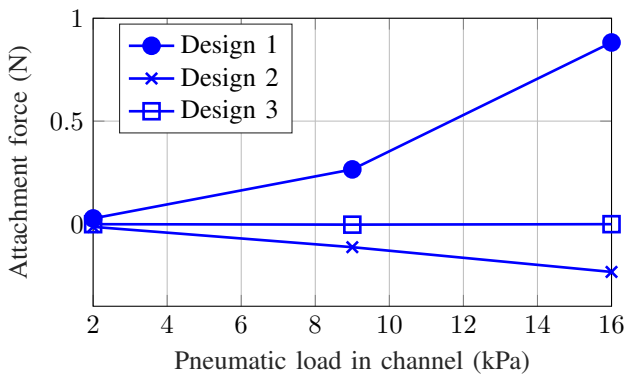

Fig. 4. Three representative behaviors observed for the simulated suction cup designs at the selected pneumatic loads. Design 1 has R = 2.5, H1 = 1 mm, H2 = 4 mm, H3 = 1 mm, H4 = 1 mm, and W = 1.3 mm. Design 2 has R = 2.5, H1 = 4 mm, H2 = 1 mm, H3 = 1 mm, H4 = 1 mm, and W = 1.3 mm. Design 3 has R = 1, H1 = 2.5 mm, H2 = 2 mm, H3 = 1 mm, H4 = 1.5 mm, and W = 1 mm.

Aspect Ratio (R): Given that slender suction cups are likely to better conform inside tubular environments, such as the gastrointestinal tract, compared to circular ones, aspect ratios of 1, 1.5, 2, and 2.5 were selected for our study.

Thicknesses (H1, H2, H3, H4): The total height of the suction cup was constrained to be 7 mm to ensure that the suction cup would easily fit into both ports and tight spaces in natural orifices while attached to the surgical tools. The minimum value of layer thickness was selected to be 1 mm, and the maximum value was defined such that the total thickness, when combined with the minimum values of all other height parameters, would equal the total desired height of the suction cup.

Channel Width (W): Channel widths of 1 mm, 1.15 mm, and 1.3 mm were investigated. The minimum and maximum values ensure that both the channel width and wall thickness between the channels remain within fabrication limits.

Number of revolutions (N): The number of revolutions of the spiral channel was 2.75 for the entire design set.

Material: The material selected for the suction cup is Ecoflex 00-30, a soft silicone rubber, which we model using the hyperelastic Yeoh model with $C_1 = 17$ kPa, $C_2 = 0.2$ kPa, and $C_3 = 0.023$ kPa [22]. We used a Poisson's ratio of 0.49 in our simulations to mimic the incompressibility of the material [23].

Input pneumatic loads of 2 kPa, 9 kPa, and 16 kPa were selected as representatives for small, medium, and large applied loads. Larger loads were not considered in order to prevent ballooning effects [24] caused by large strains. A total of 1008 suction cup designs were obtained based on the combination of all design parameters under the defined constraints. The entire design set was used for the FEA optimization study on a rigid substrate at the 3 selected pneumatic loads, for a total of 3024 designs. The time required to complete the study was 61 hours on an Intel(R) Core(TM) i7-8700K CPU with 16 GB RAM.

B. Optimization Study Results

The attachment forces generated based on the three different pneumatic loads were analyzed for the set of studied suction cup designs. We observed three distinct behaviors (Fig. 4), as illustrated by Design 1, Design 2, and Design 3, which were later qualitatively confirmed experimentally. For Design 1, which is also the best performing design, the attachment force increases with the increase in pneumatic load. The attachment force produced by Design 2, on the other hand, decreases with the increase in pneumatic load. This is due to the fact that for Design 2, the suction cup's main body bends in the direction of the substrate, rather than away from it like for Design 1, resulting in a decrease in the volume of the vacuum chamber with an increase in pneumatic load. Finally, the attachment force produced by Design 3 remains relatively unchanged across the three studied pneumatic loads because of the inability of applied pneumatic loads to change the volume of the vacuum chamber. Since it is desirable for the suction cup to generate a large attachment force, the designs that behaved similarly to Design 2 and Design 3 — which generated attachment forces close to or less than 0 N across all three pneumatic loads — did not meet the needs of our intended applications. For the designs that exhibited behavior similar to that of Design 1, the maximum attachment force was generated at the maximum pneumatic load, enabling us to select the best design from the simulation performed at the largest load (16 kPa).

The impact of individual design parameters on the suction cup's performance can be inferred from the optimization study results shown in Fig. 5 for the 1008 designs simulated with an input pneumatic load of 16 kPa. This plot shows each design represented by lines connecting the dimensions of the individual design parameters and the resulting values of F (generated attachment force) for that design. The lines are color coded based on the force generated, where the best performing design is shown in black, and the green, blue, and red lines represent high, medium, and low force values, respectively. It can be seen that the performance improved with larger H2 values, which corresponds to a larger volume of the spiral channels. Larger values of H1 led to decreased performance, possibly due to the fact that larger values of H1 means it is more difficult for suction cups to bend away from the substrate given smaller heights of other layers. The performance also worsened with larger values of H4, and the effect of H3 is not clearly evident from the results.

The best performing design at a pneumatic load of 16 kPa had an aspect ratio of 2.5, channel width of 1.3 mm, and heights of 1 mm, 4 mm, 1 mm, and 1 mm for H1, H2, H3, and H4, respectively.

IV. Experimental Evaluations

In this section, we start by fabricating the best performing design obtained from our optimization study. We then characterize its performance and compare it to results from our simulations, on both rigid and soft substrates. Finally,

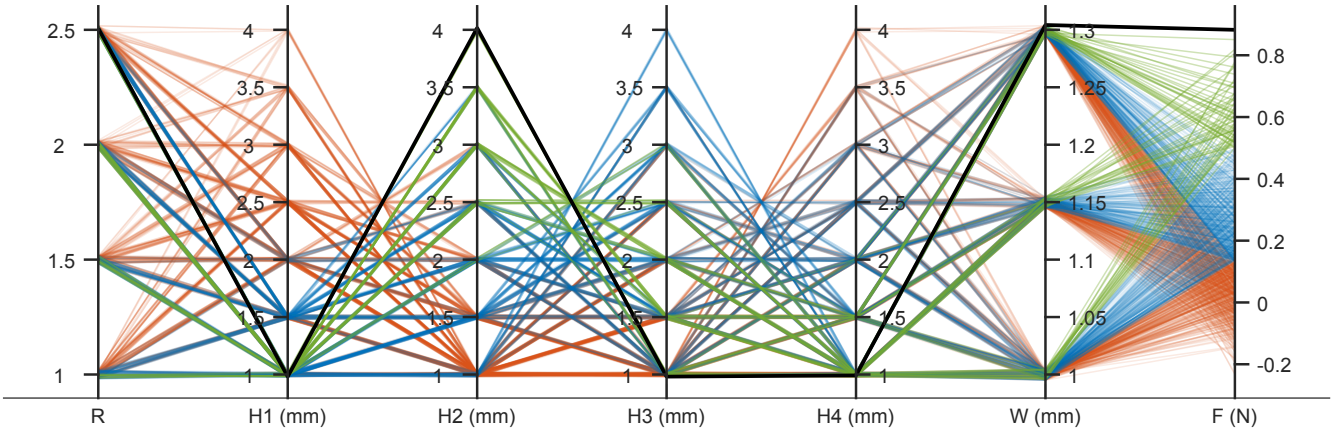

Fig. 5. Results showing parameter dimensions and generated attachment force for 1008 designs at the pneumatic load of 16 kPa on a rigid substrate. Each design is represented by lines connecting the dimensions of individual geometric parameters and corresponding values of F. The lines are color coded based on the anchoring force (F) generated for the studied designs, where the best performing design is shown in black, designs producing F between 0.860 N and 0.496 N are shown in green, those producing F between 0.496 N and 0.133 N are shown in blue, and designs producing F below 0.133 N are shown in orange.

we evaluate the capacity of our suction cup to resist external loads, and demonstrate its use on live porcine tissues.

A. *Fabrication*

Suction cups are fabricated using Ecoflex 00-30. The two part liquid mixture is combined with a 1:1 weight ratio, degassed using a vacuum container, and poured into 3-D printed molds, as seen in Fig. 6a. The liquid mixture is left to cure for 3 hours at room temperature before being removed from the molds. Mold 1 consists of the spiral channel pattern, and the associated Part 1 consists of a negative spiral space (Fig. 6b), which will eventually act as the pneumatic channel. Mold 2 is used to fabricate the base of the suction cup, and the associated Part 2 consists of the vacuum chamber and a thin surrounding lip. The two cured parts are then attached together with a thin layer of Ecoflex 00-30 (Fig. 6c) and left to cure for 3 hours. Finally, a silicone tube for supplying air to the pneumatic channel is attached using a silicone adhesive (Smooth-on Sil-poxy), resulting in a final functional suction cup, as shown in Fig. 6d.

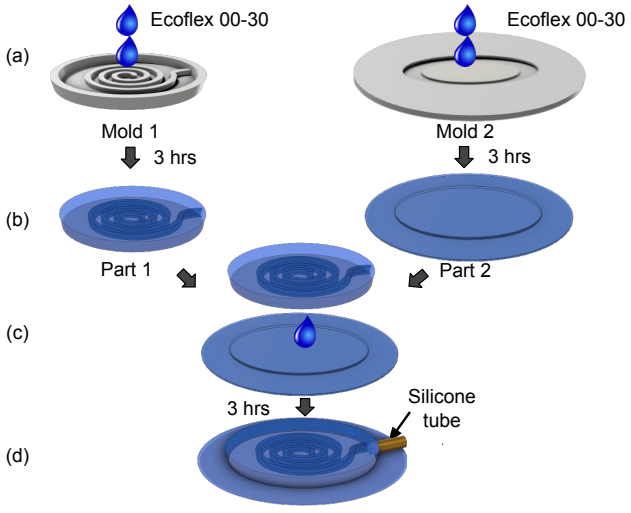

Fig. 6. The process for fabricating a positive-pressure actuated suction cup includes (a) pouring Ecoflex 00-30 into the two molds, (b) removing the two soft parts after they are cured, (c) assembling the two parts together using Ecoflex 00-30, and (d) attaching a silicone tube used for supplying air to the pneumatic channel.

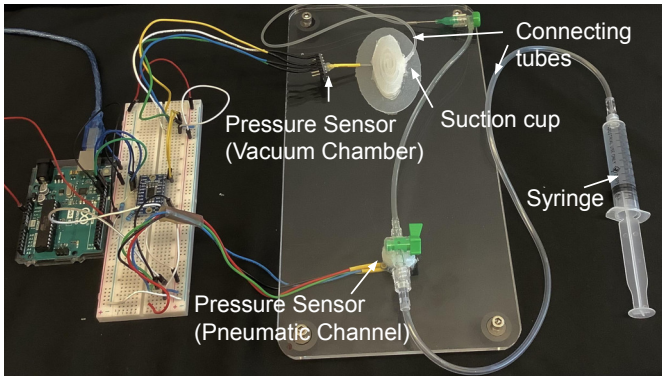

(a)

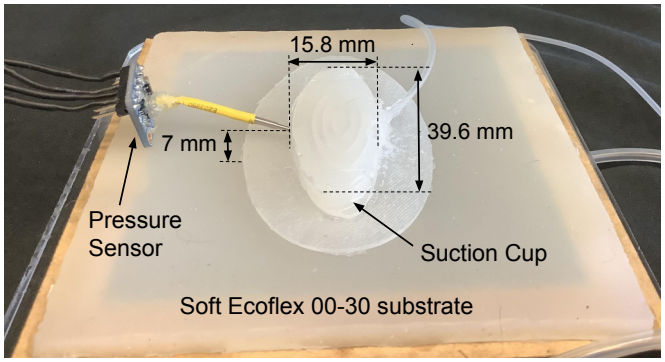

(b)

Fig. 7. (a) Experimental setup for measuring the suction cup behavior and comparing it to that predicted by the FEA simulations on both rigid and (b) soft substrates.

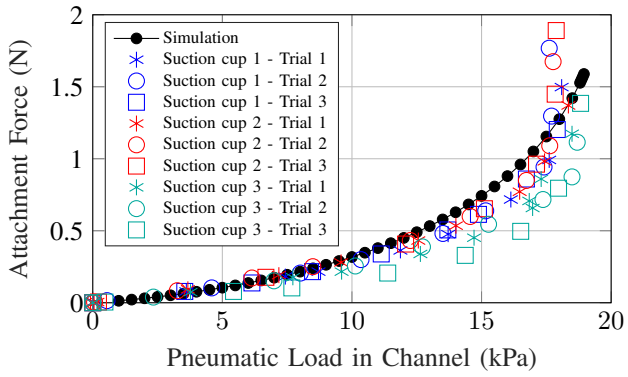

(a)

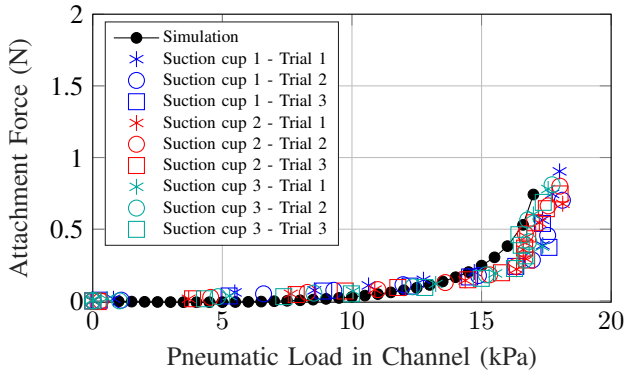

(b)

Fig. 8. Suction cup behavior predicted by FEA simulations versus experimental results for (a) rigid and (b) soft substrates.

B. Model Validation on Rigid and Soft Substrates

Experimental evaluations were conducted using the setup shown in Fig. 7 in order to measure and compare the performance of the selected suction cup with that obtained from the developed finite element model. Pressure sensors (Adafruit MRPLS) were used to measure the output pneumatic load in the vacuum chamber and the input pneumatic load, which was manually applied using a 12 mL syringe.

This experiment was performed on both a rigid and a soft substrate. The rigid substrate was made out of a thick acrylic sheet (Fig. 7a). The soft substrate was designed to mimic the properties of live tissue and was made from a 120 mm $\times$ 120 mm $\times$ 5 mm piece of Ecoflex 00-30 mounted on an acrylic frame (Fig. 7b). Ecoflex 00-30 was selected since it has been found to have a similar stress distribution trend and shear modulus as published values for porcine muscle [25] and has well-known material properties [22]. The use of live tissues themselves is challenging due to large variances in their model parameters and unpredictability between different specimens [26].

Three suction cups with the same selected parameters were fabricated, and experiments were repeated three times per substrate for each suction cup. The attachment forces were then calculated based on the measured pneumatic load generated using Eq. (1) and Eq. (2). As seen in Fig. 8a and 8b, behavior of the fabricated suction cups matched that predicted in the simulation for both the rigid and soft substrates, respectively. Although there were slight differences in behavior among the suction cups, which is expected for structures manually fabricated from soft materials, the general trends remained consistent. The attachment force generated increased almost linearly with an increase in the pneumatic load in the channel until a critical pneumatic load – approximately 17 kPa and 16 kPa for the rigid and soft substrate, respectively – was reached. Beyond this load, there was an exponential increase in the generated force, an excessive ballooning that could lead to structural damage, and an increase in the difficulty to control the generated force.

For the same set of initial conditions, we found that the attachment force generated on the soft substrate was smaller than that on the rigid substrate. This phenomenon can be explained by the smaller increase in vacuum chamber volume (ΔV) on soft substrates than that on rigid substrates. This decrease in ΔV occurs due to the deformation of the soft substrate during suctioning, as represented in Fig. 1 and Fig. 2.

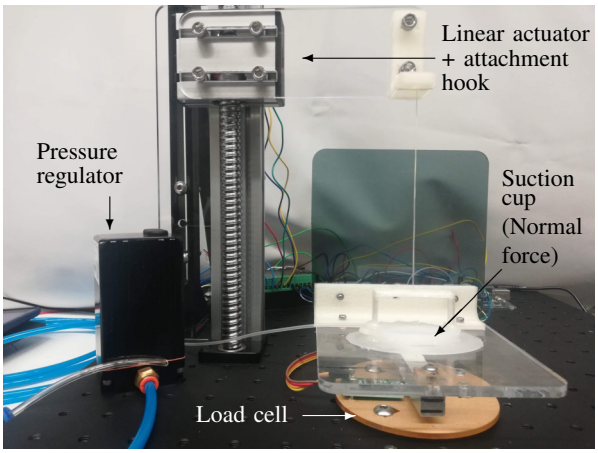

(a)

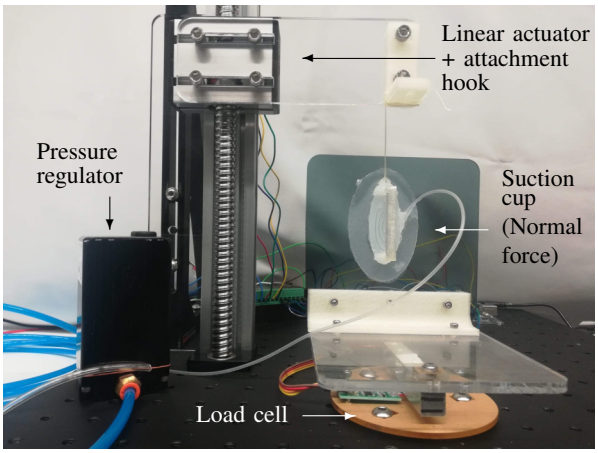

(b)

Fig. 9. Experimental setup for measurement of maximum (a) normal forces and (b) shear forces that the suction cups can resist.

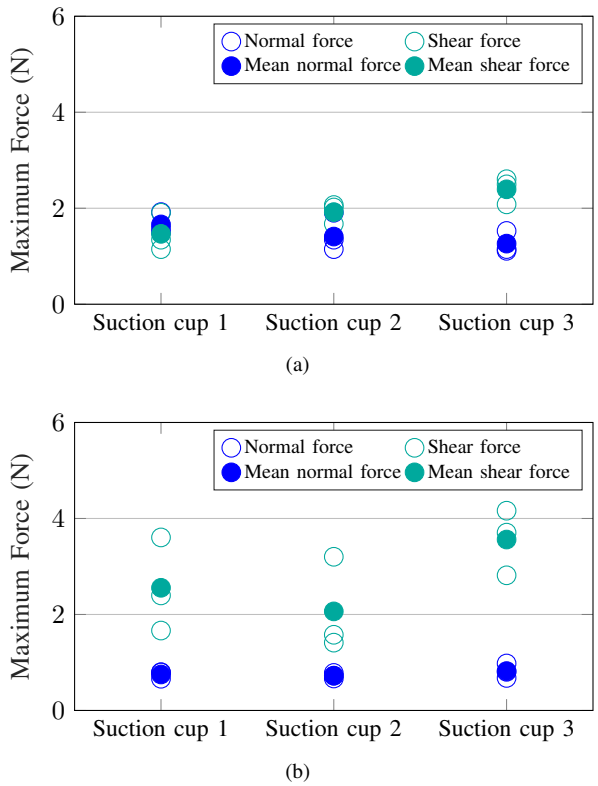

Fig. 10. Results showing the maximum normal and shear forces resisted during each trial, along with the mean of these maximum forces, as measured on (a) a rigid substrate and (b) a soft substrate.

C. Performance Evaluation with External Loads

The goal of this experiment was to measure the maximum normal and shear forces that the suction cups can resist. As shown in Fig. 9, a linear actuator consisting of a stepper motor (Nema 23) and a lead screw was used to pull on the suction cups in a controlled manner. The suction cups were mounted horizontally and vertically for normal (Fig. 9a) and shear (Fig. 9b) force measurement, respectively, on both rigid and soft substrates. The pull rate was fixed at 4 mm/s, and the pulling force was measured using a load cell (Makerhawk digital load cell with HX711 ADC module). A pressure regulator (QB1X) was used to control the pneumatic load, which was fixed at 16 kPa. Three experiments for each suction cup were performed and repeated on both the rigid and soft substrates.

The results for the maximum normal and shear forces that the suction cups could resist are shown in Fig. 10. The average peak normal force that the suction cups could resist was 1.45 ± 0.28 N and 0.77 ± 0.10 N for the rigid and soft substrates, respectively. It was also observed that the seal between the suction cups and the substrates was easily disturbed when the suction cups were pulled in the normal direction, resulting in their premature failure through detachment.

The shear forces were measured along the direction of the major axis of the oval suction cup. The average peak shear forces that the suction cups could resist was 1.93 ± 0.48 N and 2.73 ± 1.02 N for the rigid and soft substrates, respectively. The seal between the suction cups and the substrates was less vulnerable to detachment when under a shear force due to friction.

When the suction cups are pulled away from the substrate during the application of external forces (normal and shear), the volume of the vacuum chamber increases beyond the change due to the actuation mechanism itself. This increase in volume continues until the suction cups detach. The larger change in volume results in the suction cups resisting larger external forces than predicted by Eq. 2, which gives the attachment force in the absence of external forces.

V. In-Vivo Demonstration

Finally, the selected suction cup design was tested on live porcine tissues, namely liver and spleen, as a preliminary demonstration towards more clinically relevant evaluations. The federal and institutional guidelines for the care and use of laboratory animals were followed (IACUC protocol: S06253). A force gauge (Baoshishan Z-50N) was used to measure the forces (normal and shear) that the suction cup could resist when actuated on the tissues. As shown in Fig. 11, when placed on the liver, the suction cup could resist up to 3.34 N and 1.59 N of normal and shear forces, respectively, without experiencing the ballooning effect. Similarly, when placed on the spleen, it could resist 1.05 N

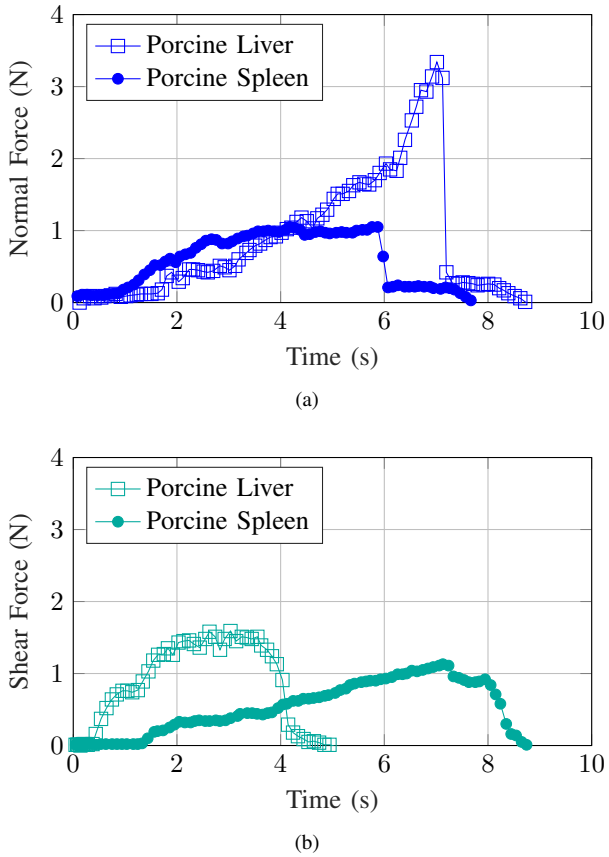

Fig. 11. Results showing (a) normal forces and (b) shear forces the suction cup resisted on porcine tissues.

and 1.13 N of normal and shear forces, respectively. The differences in performance between the two tissues may be due to differences in surface and mechanical properties of the tested tissues. For example, differences in the amount of viscous fluid present, the concavity of the tissue, and the stiffness may all play a role, and further study is required to fully characterize the possible phenomena. These preliminary tests on live tissues demonstrate the potential of the proposed positive-pressure suction cups for anchoring to tissues during surgical procedures.

VI. Conclusion

In this paper, a finite element model that enables the simulation of the behavior of positive-pressure actuated suction cups on both rigid and soft substrates was presented. The geometry of a positive-pressure actuated suction cup was optimized using the developed model to maximize its attachment force for use in MIS in order to stabilize flexible surgical tools. Experiments were conducted to successfully validate the developed model and to assess the ability of the selected suction cup design to resist external forces on both rigid and soft substrates. An in-vivo demonstration on live porcine tissues was conducted to showcase the applicability of these suction cups as anchoring units for MIS.

As a continuation of this work, multiple units could be integrated to create a functional soft system to meet the anchoring demands of surgery. Future work could also expand the study to include different channel designs and their effects on overall performance. The suction cup design can also be modified to include features, such as micro patterns and switchable adhesives at the interface between the suction cup and the tissue, which could increase the maximum attachment force by improving the seal. The vacuum chamber design can also be modified to restrict the deformation of soft substrates in the chamber during actuation. Finally, because deformation of the soft substrate can be correlated to the pressure generated in the vacuum chamber, future research can leverage this ability for studying the material properties of different soft substrates.

References

[1] B. Bahr, Y. Li, and M. Najafi, "Design and suction cup analysis of a wall climbing robot," *Computers & electrical engineering*, vol. 22, no. 3, pp. 193–209, 1996.

[2] Y. Yoshida and S. Ma, "Design of a wall-climbing robot with passive suction cups," in *2010 IEEE International Conference on Robotics and Biomimetics*. IEEE, 2010, pp. 1513–1518.

[3] H. Iwasaki, F. Lefevre, D. D. Damian, E. Iwase, and S. Miyashita, "Autonomous and reversible adhesion using elastomeric suction cups for in-vivo medical treatments," *IEEE Robotics and Automation Letters*, vol. 5, no. 2, pp. 2015–2022, 2020.

[4] A. Koivikko, D.-M. Drotlef, M. Sitti, and V. Sariola, "Magnetically switchable soft suction grippers," *Extreme Mechanics Letters*, vol. 44, p. 101263, 2021.

[5] S. Song, D.-M. Drotlef, D. Son, A. Koivikko, and M. Sitti, "Adaptive self-sealing suction-based soft robotic gripper," *Advanced science*, vol. 8, no. 17, p. 2100641, 2021.

[6] D. Ge, T. Matsuno, Y. Sun, C. Ren, Y. Tang, and S. Ma, "Quantitative study on the attachment and detachment of a passive suction cup," *Vacuum*, vol. 116, pp. 13–20, 2015.

[7] M. Follador, F. Tramacere, and B. Mazzolai, "Dielectric elastomer actuators for octopus inspired suction cups," *Bioinspiration & biomimetics*, vol. 9, no. 4, p. 046002, 2014.

[8] S.-M. Kirsch, F. Welsch, M. Schmidt, P. Motzki, and S. Seelecke, "Bistable sma vacuum suction cup," in *ACTUATOR 2018; 16th International Conference on New Actuators*. VDE, 2018, pp. 1–4.

[9] P. Cheng, Y. Ye, J. Jia, C. Wu, and Q. Xie, "Design of cylindrical soft vacuum actuator for soft robots," *Smart Materials and Structures*, vol. 30, no. 4, p. 045020, 2021.

[10] Y. Tang, Q. Zhang, G. Lin, and J. Yin, "Switchable adhesion actuator for amphibious climbing soft robot," *Soft robotics*, vol. 5, no. 5, pp. 592–600, 2018.

[11] Z. Zhakypov, F. Heremans, A. Billard, and J. Paik, "An origami-inspired reconfigurable suction gripper for picking objects with variable shape and size," *IEEE Robotics and Automation Letters*, vol. 3, no. 4, pp. 2894–2901, 2018.

[12] A. Bamotra, P. Walia, A. V. Prituja, and H. Ren, "Fabrication and characterization of novel soft compliant robotic end-effectors with negative pressure and mechanical advantages," in *2018 3rd International Conference on Advanced Robotics and Mechatronics (ICARM)*. IEEE, 2018, pp. 369–374.

[13] E. S. Dellon, J. S. Hawk, I. S. Grimm, and N. J. Shaheen, "The use of carbon dioxide for insufflation during gi endoscopy: a systematic review," *Gastrointestinal endoscopy*, vol. 69, no. 4, pp. 843–849, 2009.

[14] W. Mouton, J. Bessell, K. Otten, and G. Maddern, "Pain after laparoscopy," *Surgical endoscopy*, vol. 13, no. 5, pp. 445–448, 1999.

[15] E. Guan, Y. Ge, J. Liu, W. Yan, and Y. Zhao, "Piezoelectric micropump suction cup design and research on the optimal static driving characteristics," in *International Conference on Intelligent Robotics and Applications*. Springer, 2017, pp. 26–38.

[16] H. Tsukagoshi and Y. Osada, "Soft hybrid suction cup capable of sticking to various objects and environments. actuators 2021, 10, 50," 2021.

[17] J. A. Sandoval, S. Jadhav, H. Quan, D. D. Deheyn, and M. T. Tolley, "Reversible adhesion to rough surfaces both in and out of water, inspired by the clingfish suction disc," *Bioinspiration & biomimetics*, vol. 14, no. 6, p. 066016, 2019.

[18] M. K. Choi, O. K. Park, C. Choi, S. Qiao, R. Ghaffari, J. Kim, D. J. Lee, M. Kim, W. Hyun, S. J. Kim *et al.*, "Cephalopod-inspired miniaturized suction cups for smart medical skin," *Advanced healthcare materials*, vol. 5, no. 1, pp. 80–87, 2016.

[19] C. Tawk and G. Alici, "Finite element modeling in the design process of 3d printed pneumatic soft actuators and sensors," *Robotics*, vol. 9, no. 3, p. 52, 2020.

[20] A. Gao, N. Liu, M. Shen, M. EMK Abdelaziz, B. Temelkuran, and G.-Z. Yang, "Laser-profiled continuum robot with integrated tension sensing for simultaneous shape and tip force estimation," *Soft Robotics*, vol. 7, no. 4, pp. 421–443, 2020.

[21] Z. Wang, T. Wang, B. Zhao, Y. He, Y. Hu, B. Li, P. Zhang, and M. Q.-H. Meng, "Hybrid adaptive control strategy for continuum surgical robot under external load," *IEEE Robotics and Automation Letters*, vol. 6, no. 2, pp. 1407–1414, 2021.

[22] D. Steck, J. Qu, S. B. Kordmahale, D. Tscharnuter, A. Muliana, and J. Kameoka, "Mechanical responses of ecoflex silicone rubber: Compressible and incompressible behaviors," *Journal of Applied Polymer Science*, vol. 136, no. 5, p. 47025, 2019.

[23] Y.-D. Kwon, S.-B. Kwon, X. Lu, and H.-W. Kwon, "A finite element procedure with poisson iteration method adopting pattern approach technique for near-incompressible rubber problems," *Advances in Mechanical Engineering*, vol. 6, p. 272574, 2014.

[24] Y. Elsayed, A. Vincensi, C. Lekakou, T. Geng, C. Saaj, T. Ranzani, M. Cianchetti, and A. Menciassi, "Finite element analysis and design optimization of a pneumatically actuating silicone module for robotic surgery applications," *Soft Robotics*, vol. 1, no. 4, pp. 255–262, 2014.

[25] J. L. Sparks, N. A. Vavalle, K. E. Kasting, B. Long, M. L. Tanaka, P. A. Sanger, K. Schnell, and T. A. Conner-Kerr, "Use of silicone materials to simulate tissue biomechanics as related to deep tissue injury," *Advances in skin & wound care*, vol. 28, no. 2, pp. 59–68, 2015.

[26] K. Lister, Z. Gao, and J. P. Desai, "Development of in vivo constitutive models for liver: Application to surgical simulation," *Annals of biomedical engineering*, vol. 39, no. 3, pp. 1060–1073, 2011.